

Fatigue Fracture Behavior of ARB Processed Aluminum

Hiromoto Kitahara^{1, a}, Takuya Horike^{1, b}, Masayuki Tsushida^{1, c}
Shinji Ando^{1, d} and Nobuhiro Tsuji^{2, e}

¹ Department of Materials Science and Engineering, Kumamoto University,
2-39-1, Kurokami, Kumamoto 860-8555, Japan

² Department of Materials Science and Engineering, Kyoto University,
Yoshida Honmachi, Sakyo-ku, Kyoto 606-8501, Japan

^a kitahara@msre.kumamoto-u.ac.jp, ^b 083d8425@st.kumamoto-u.ac.jp,

^c tsushida@tech.eng.kumamoto-u.ac.jp, ^d shinji@msre.kumamoto-u.ac.jp,

^e nobuhiro.tsuji@ky5.ecs.kyoto-u.ac.jp

Keywords: ultrafine grain, fatigue crack propagation, threshold stress intensity factor range

Abstract. Fatigue crack propagation behaviors of ultrafine grained (UFG) Al sheets fabricated by the accumulative roll bonding (ARB) process were investigated. The ARB process was carried out up to 6 cycles (equivalent strain, $\varepsilon_{eq}=4.8$). The ARB processed sheet had lamellar boundary structure elongated to rolling direction of the sheet. The mean spacing of the boundaries was 182 nm. The tensile strength of the starting Al sheet increased after the 6-cycle of the ARB. Fatigue crack growth tests were performed to clarify the crack growth rate and threshold stress intensity factor range for crack growth (ΔK_{th}). The fatigue crack profile in the ARB processed sheet differs from that in the starting Al sheet. The ΔK_{th} of the ARB processed sheet was smaller than that of the starting sheet. The ΔK_{th} of Al would decrease with decreasing the crack closure phenomena after the 6-cycle of the ARB. The fatigue crack growth rate test shows that the critical load for starting to propagate the fatigue crack and the fatigue crack growth rate decreased by ultrafine grain refinement.

Introduction

The severe plastic deformation (SPD) process, which mechanically can induce the large strain (equivalent strain: $\varepsilon_{eq} > 4.0$) into materials, can fabricate bulk ultrafine grained (UFG) materials. The UFG materials whose mean grain size is smaller than 1 μm exhibit the high mechanical properties superior to conventional materials with coarse grains. Various kinds of the SPD processes have been developed, and the typical processes are accumulative roll bonding (ARB) [2-4], equal channel angler pressing (ECAP) [1-3]. The SPD processes actually succeeded in producing bulk UFG materials with nano- or sub-micro-meter sized grains in various kinds of metallic materials, and the UFG materials actually exhibited high tensile strength [1-4]. It is, therefore, expected that the UFG materials fabricated by the SPD process show high fatigue properties. Fatigue data of the UFG materials are also required for practical use as structural materials.

The fatigue properties of the UFG materials fabricated by the SPD process have been reported: fatigue crack growth rate ($da/dN-\Delta K$) [5-7], fatigue strength and fatigue life (S-N curve) [8], etc. Although fatigue data of the UFG materials has been reported, the most of the data were obtained from the UFG materials fabricated by the ECAP. It is expected that the fatigue fracture behavior depends on the SPD process, because it generally depends on the microstructure. For example, the deformation process of the ARB and ECAP is totally different. However, the fatigue data of the UFG materials fabricated by other SPD techniques is still quite limited [9]. Therefore, further fatigue data is required to understand the universal fatigue fracture behavior of the UFG materials. This study was carried out to clarify the fatigue crack propagation behavior in the UFG Al fabricated by the ARB process.

Experimental Procedure

Commercial purity Al (99.11% purity) sheets 1mm thick were used in this study. The starting sheets were strain-hardened and then partially annealed (H24 temper), and they were subjected to the ARB process to fabricate the UFG Al sheet. In the ARB process, the starting sheet 1mm thick was stacked to be 2 mm thick after degreasing and wire brushing the surface, and then provided to the 50% roll bonding. This is one cycle of the ARB. The cycle was repeated up to 6 cycles, and the total equivalent strain accumulated in the ARB processed sheet was 4.8. The rolling was done without lubricant by the use of a two high mill with a roll diameter of 310 mm at room temperature.

Fatigue crack growth tests according to ASTM standard E647 were carried out at a stress ratio $R=0.1$ with an electro servo hydraulic fatigue testing machine operated at frequency of 10Hz at room temperature. The direction of the crack propagation is perpendicular to the rolling direction (RD) of the sheets. Tensile tests were also carried out to evaluate static strength. Microstructure and fracture surfaces before and after the fatigue tests were observed by SEM, SEM/EBSD and TEM.

Results and Discussion

Figure 1 shows a TEM image of the ARB processed sheet. The structure was observed from transverse direction (TD) of the sheet. The ARB processed sheet had lamellar boundary structure elongated to RD. The mean spacing of the boundaries from TEM observation was 182 nm. From the SEM/EBSD observation, many high- and low-angle boundaries induced by 6-cycle of the ARB, and the mean spacing of the high angle boundaries was 271nm. Anyway, the UFG Al sheet having ultrafine grain smaller than $1\mu\text{m}$ can be obtained by the 6-cycle of the ARB. Figure 2 shows the nominal stress-strain curves of the starting and ARB processed sheets. The 0.2% proof stress and tensile strength significantly increased by 6-cycle of the ARB, although the elongation decreased. The 0.2% proof stress of the ARB processed sheet was 202 MPa, which was about 1.7 times higher than that of the starting sheet (121MPa).

Figure 3 shows optical micrographs of the fatigue crack propagation profiles in the (a) starting and (b) ARB processed sheets during fatigue crack growth tests. Fatigue cracks initiated from the notch on the left side, and they started to propagate to the right. In the starting sheet, the fatigue crack propagates macroscopically straight but with small zigzag pattern. On the other hand, the smooth fatigue crack profile without the zigzag pattern was observed in the ARB processed sheet. The similar change in the fatigue crack profile has been reported in some papers [7, 9]. In low carbon steel, the change occurred after the ECAP [7]. On the other hand, Kitahara *et al.* [9] has been reported that the fatigue crack profile changes after the 2-cycle of the ARB at the least in the commercial purity Ti. The 2-cycle of the ARB is not the SPD ($\varepsilon_{\text{eq}} > 4.0$), because of conventional 75% rolling (i.e., $\varepsilon_{\text{eq}} = 1.6$).

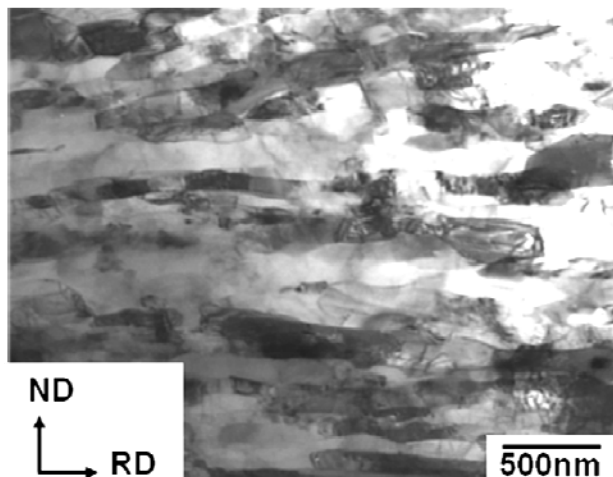


Fig.1 TEM image of the sheet ARB processed by 6-cycle. Observed from transverse direction (TD) of the sheet.

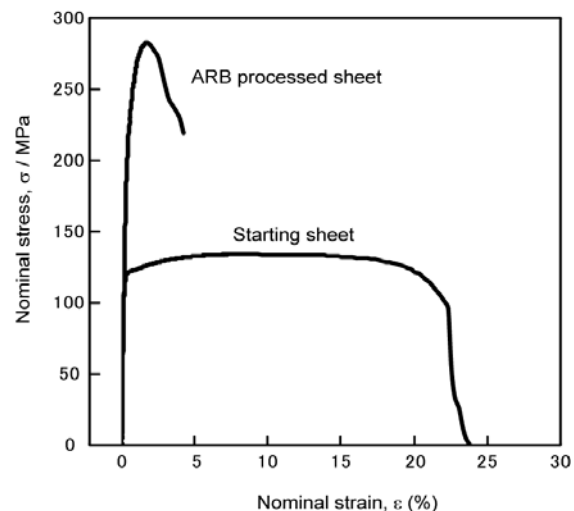


Fig.2 Nominal stress-strain curves of the starting sheet and the sheet ARB processed by 6-cycle.

Therefore, the changes are not limited in the SPD processed specimens.

The log-log plot of the stress intensity factor range (da/dN) versus the stress intensity factor range (ΔK) is shown in Fig.4. In this study, the minimum ΔK was used as the ΔK_{th} (the threshold stress intensity factor range for crack growth). The ΔK_{th} of the ARB processed sheet ($2.3 \text{ MPam}^{1/2}$) was lower than that of the starting sheet. The decreasing ΔK_{th} has been reported in ECAPed-Al alloys [5, 6], low carbon steel [7] and ARB processed Ti sheets [9]. It has been expected that the crack closure phenomena decreased after the ECAP and the ARB because of the strengthening by the ultrafine grain refinement after the SPD. Therefore, the ΔK_{th} of Al would decrease with decreasing the crack closure phenomena after the 6-cycle of the ARB. In Fig.4, the curves have a linear part where the crack propagation is stable above the ΔK_{th} , i.e., Paris's law region. The slope of a linear part decreased after the 6-cycle of the ARB. The decreasing in the slope shows that the ARB specimen has long fatigue life from the viewpoint of the damage tolerance design. The fatigue crack growth rate test shows that the fatigue crack of the ARB processed sheet starts to propagate at the low load and but its rate is slower than the starting sheet.

Figure 5 shows SEM images of the typical fracture surfaces of the (a) starting sheet and (b) ARB processed sheet after the fatigue crack growth test. Fatigue crack propagates from left to right in the micrographs. The stress intensity factor range of the observed area corresponds to around the ΔK_{th} : $3.3 \text{ MPam}^{1/2}$ and $2.3 \text{ MPam}^{1/2}$ for the starting and ARB processed sheets, respectively. The rough fracture surfaces were observed in both the starting and ARB processed sheets. Although the size of the patterns was different, the morphology of the fracture surface of the ARB processed sheet was similar to that of the starting sheet. The different size of the patterns would depend on the grain size.

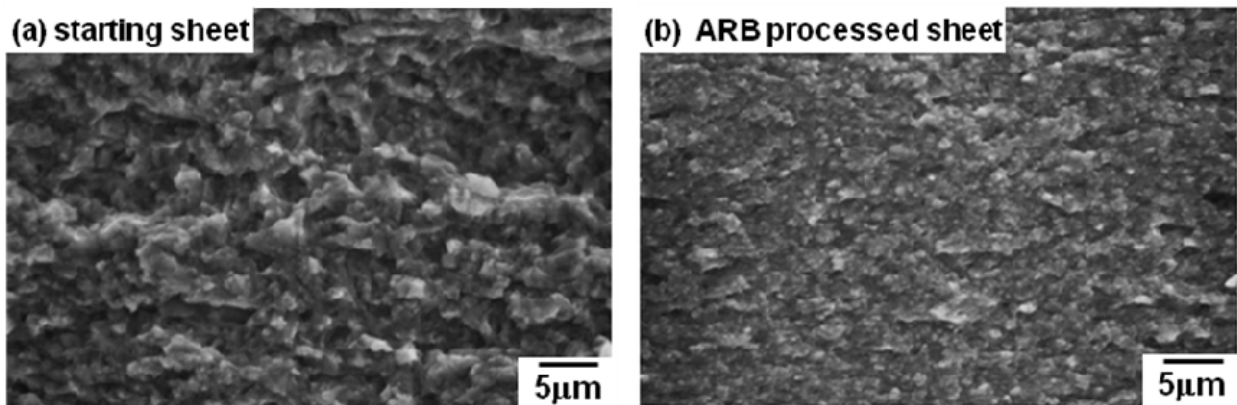


Fig.5 SEM images of the fracture surfaces of the (a) starting sheet and (b) ARB processed sheet.

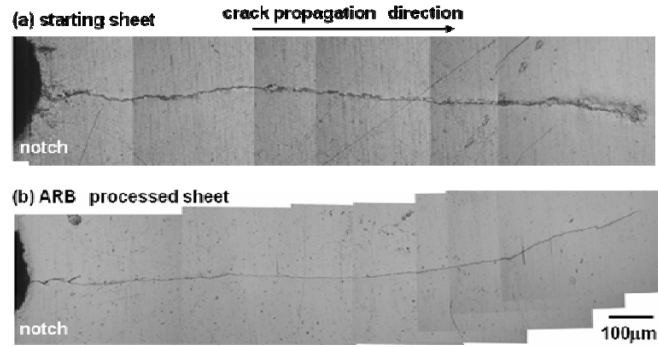


Fig.3 Fatigue crack profiles of the starting and ARB processed sheets.

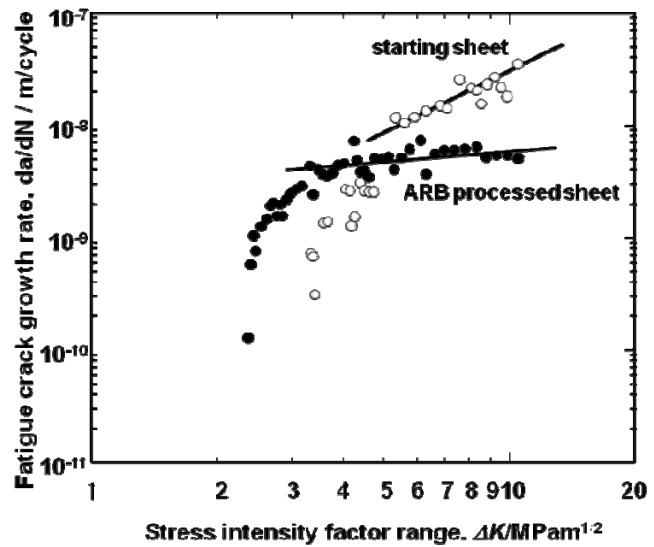


Fig.4 Relationship between fatigue crack growth rate and stress intensity factor range of the starting sheet and the sheet ARB processed by 6-cycle.

Further systematic investigations on the relationship between fatigue data and the microstructural characteristics are required, and it will be carried out in our future studies.

Summary

The fatigue crack propagation behaviors in the commercial pure Al sheets severely deformed by the accumulative roll bonding (ARB) process were investigated. ARB processed sheet has the lamellar boundary structure, and its spacing was 182nm. The tensile strength of the ARB processed sheet was 202 MPa, which was about 1.7 times higher than that of the starting sheet. The fatigue crack profile in the ARB processed sheet differs from that in the starting Al sheet. Threshold stress intensity factor range (ΔK_{th}) decreased after the ARB. The ΔK_{th} would decrease with decreasing the crack closure phenomena after the 6-cycle of the ARB. The rough fracture surface was observed in both the starting and ARB processed sheets. Although the size of the patterns was different, the morphology of the fracture surface of the 6-cycle specimen was similar to that of the starting sheet. The different size of the patterns would depend on the grain size.

References

- [1] R.Z.Valiev, R. K. Isalamgliev, I.V. Alexandrov: Prog. in Mater. Sci. Vol.45 (2000),p. 103
- [2] N.Tsuji, Y.Saito, S.H.Lee, Y.Minamino: Adv. Eng. Mater. Vol.5 (2003),p. 338
- [3] R.Z.Valiev, Y.Estrin, Z.Horita, T.G. Langdon, M.J. Zehetbauer, Y.T. Zhu: JOM Vol.58 (2006) p.33
- [4] Y.Saito, N.Tsuji, H.Utsunomiya, T.Sakai: Acta Mater. Vol.47 (1999),p.579
- [5] A.Vinogradov, S.Nagasaki, V.Patlan, K.Kitagawa, M.Kawazoe: Nanostruct. Mater. Vol.11 (1999), p. 925
- [6] C.S.Chung, J.K.Kim, H.K.Kim, W.J.Kim: Mater. Sci. Eng. Vol.A337 (2002), p.39
- [7] H.K.Kim, M.I. Choi, C.S. Chung, D.H.Shin: Mater. Sci. Eng. Vol.A340 (2003) p.243
- [8] A.Vinogradov, A.Washikita, K.Kitagawa, V.I.Kopylov: Mater. Sci. Eng. Vol.A349 (2003), p.318
- [9] H.Kitahara, K.Uchikado, J.Makino, N.Iida, M.Tsushida, N.Tsuji, S.Ando and H.Tonda : Mater.Trans. Vol.49 (2008), p. 64